Turkish Journal of Electrical Engineering & Computer Sciences

http://journals.tubitak.gov.tr/elektrik/

Research Article

Turk J Elec Eng & Comp Sci
(2020) 28: 2821 – 2837

doi:10.3906/elk-1912-126

Diagnosis of speed sensor faults in an induction machine based on a robust adaptive super-twisting observer

Mohammed Zakaria KARI[1]*, Abdelkader MECHERNENE[1], Sidi Mohammed MELIANI[2], Ibrahim GUENOUNE[3]

[1]Laboratoire d'Automatique de Tlemcen (LAT), University of Tlemcen, Tlemcen, Algeria
[2]Manufacturing Engineering Laboratory of Tlemcen (MELT), University of Tlemcen, Tlemcen, Algeria
[3]Inteva Products, Sully Loire, France

Received: 20.12.2019 • **Accepted/Published Online:** 15.05.2020 • **Final Version:** 25.09.2020

Abstract: The present paper aims to determine a robust sensor fault-tolerant controller based on fuzzy logic using a robust adaptive super-twisting observer for the control of an induction machine and an inverter set by a state estimation method. The speed sensor is considered in the present case. The modular structure of the fault-tolerant control (FTC) scheme allows integrating this sensor within the existing closed-loop system, and the observer can therefore be designed independently. This article presents a new method to develop a fuzzy decision system that provides fault-tolerant control. This paper also aims at detecting the mechanical speed sensor faults. The proposed approach allows the automatic reconfiguration of the system in the event of a speed sensor failure. The defective fuzzy detection system makes a transition between the speed sensor and the robust observer based on a super-twisting algorithm that ensures the continuity and stability of the system; the fuzzy detection and transition system is required to be robust to parametric variations, and must be fast enough in order to locate the defect and eventually make a transition in the event of a fault. The output of the fuzzy block is injected into the control block to ensure super-twisting speed regulation. The performance of the proposed strategy also the robustness against parameter variation are assessed by simulation thanks to Matlab/Simulink software.

Key words: Sensorless control, fuzzy supervisor, fault detection and isolation, Liyaponov theory, induction machine

1. Introduction

Nowadays, mastery of risks and operational safety occupies an important place in automated industrial systems. However, this operational safety can unfortunately be hampered by some malfunctions that may occur within the system; these misfunctions can be attributed to the complexity of that system, particularly in relation with the field control part [1]. When dealing with this issue, the manufacturers are required to develop an effective technicality of monitoring a system that should be equipped with a suitable diagnostic tool in order to detect, identify, locate, and isolate any fault that is responsible for a malfunction within a system. This helps to prevent the propagation of the problem and to limit the bad consequences that could arise from that defect; it can certainly ensure the safety of people and improve the reliability and availability of their production tools [2]. To this end, and in order to provide online monitoring of these processes. Several recent methods of faults diagnostic for induction motor have been developed (see for example [3–6]). The literature shows a great diversity of methods from different points of view. Hardware redundancy has often been used in the past but

*Correspondence: kari.mohamedzakaria@gmail.com

this generally adds complexity to the design of the system and increases its cost price. Despite the overhead of the computing time, software redundancy has become a promising alternative to hardware redundancy [1, 7]. This can be an interesting and efficient solution to this problem because it is flexible and has the capacity to evolve. Estimating the conditions or parameters of the system appears to be an appropriate and efficient tool for fault-tolerant control (FTC). Moreover, this approach is commonly recommended for the detection of defects because it induces only a very short delay in the decision-making process [7]. Its main advantage lies in its capacity to detect partial defects as compared to traditional methods which can only find the failure of the entire sensor. More specifically, this method allows for a quick detection of various types of faults, such as polarization, saturation, or complete disconnection of the system. Recently, analytical methods have become increasingly important; they have been widely used especially in the context of critical applications such as the energy systems, transport systems and industry. These methods have evolved considerably since their introduction. Using an analytical model helps better know and understand the system. The basic principle consists of collecting information on the process to be monitored, using sensors [8–10]. Comparing the actual behavior and the predicted one using the suggested model provides information that is contained in a set of defect indicator signals (residues). The temporal analysis or frequency analysis of these signals makes it possible to detect and interpret any abnormal behavior of the system in order to locate the origin of the failure. Many researchers have repeatedly proposed to exploit these techniques, and particularly those addressing linear models, by adapting electrotechnical applications. It is worth reminding that an electrotechnical system has two interesting peculiarities; first, it can be decomposed into several subsystems linked together, and second, the models used in these systems are generally linear; if they are not, they can be linearized. Studying the possible drawbacks and trying to find the appropriate solutions to the problem is a necessity in order to achieve good fault tolerant control architecture [10–12].

Furthermore, artificial intelligence techniques generally confer the capacity and power needed in solving the different problems encountered in the field of industrial systems, particularly those related to the control of electrical machines. It has been observed that using fuzzy logic represents one of the most interesting routes for the implementation of the core of the proposed fault-tolerant control (FTC) [2, 13].
A new fuzzy supervisor for fault-tolerant speed sensor for induction motors controlled by super-twisting is designed in this article. The super-twisting procedure uses the same sliding-mode. In addition, it has a finite-time convergence and is less chattering as compared to the other procedure. The function of a fuzzy supervisor is to allow a transition of the system. When a fault is detected in the speed sensor, to the rotor speed which is estimated by the adaptive super-twisting observer which in turn guarantees the continuity of the system. The system must be robust to parametric variation; it must not make any transition in case of any change in parameters and is required to be fast enough in order to detect and locate the fault and then make a transition to the speed given by the observer in the sliding mode. The paper is organized as follows. In Section 2, the mathematical models of the induction motor (IM) are first presented in the reference frame, rotating at the synchronous speed, and then in the stationary stator reference frame. Section 3 describes the principle of rotor flux orientation; the theory of super-twisting sliding modes and its application to induction motor control are also developed. Section 4 introduces the concepts of adaptive super-twisting speed and rotor flux observer. Section 5 describes the fuzzy detection and reconfiguration system proposed in this paper. In Section 6, some simulation results related to the performance of the suggested strategy of fault-tolerant control (FTC) associated with motor control are presented and discussed. Finally, Section 7 provides some comments and then gives a final conclusion.

The main objective of this work is to propose a robust and reliable detection and reconfiguration system for the detection of a speed sensor defect. The main contributions are:

- A robust proposed observer which guarantees a good estimate of the rotor speed in different areas especially at low speed (area of nonobservability);
- The fuzzy detection and reconfiguration system that guarantees the continuity of the system in presence of the several disturbances (fault, parameter variation).

The results of simulations presented in this paper clearly show these contributions.

2. Mathematical modeling of IM

2.1. Modeling of IM in the (d-q) reference frame

The mathematical model of a three-phase induction motor, established in a (d-q) reference frame that is rotating at the synchronous speed, can be expressed by means of the following nonlinear system [14]:

$$\begin{cases} \frac{di_{sd}}{dt} &= -\gamma i_{sd} + \omega_s i_{sq} + \frac{K}{T_r}\psi_{rd} + K\omega_r\psi_{rq} + \frac{1}{\sigma L_s}v_{sd} \\ \frac{di_{sq}}{dt} &= -\omega_s i_{sd} - \gamma i_{sq} + K\omega_r\psi_{rd} + \frac{K}{T_r}\psi_{rq} + \frac{1}{\sigma L_s}v_{sq} \\ \frac{d\psi_{rd}}{dt} &= \frac{L_m}{T_r}i_{sd} - \frac{1}{T_r}\psi_{rd} + (\omega_s - \omega_r)\,\psi_{rq} \\ \frac{d\psi_{rq}}{dt} &= \frac{L_m}{T_r}i_{sq} - (\omega_s - \omega_r)\psi_{rd} - \frac{1}{T_r}\psi_{rq} \\ \frac{d\omega_r}{dt} &= \frac{n_p}{J}(T_e - T_l) - \frac{B}{J}.\omega_r \end{cases} \tag{1}$$

where

$$\gamma = \left(\frac{1}{\sigma.T_s} + \frac{(1-\sigma)}{\sigma.T_r}\right); \quad K = \frac{L_m}{\sigma.L_s.L_r}; \quad T_r = \frac{L_r}{R_r}; \quad \sigma = 1 - \frac{L_m^2}{L_s.L_r}; \quad T_s = \frac{L_s}{R_s}$$

The synchronously angular speed is defined by:

$$\omega_s = \omega_r + \omega_{sl} \tag{2}$$

The electromagnetic torque is given by the following expression:

$$T_e = \frac{3}{2}\cdot\frac{n_p\cdot L_m}{L_r}\cdot(\psi_{rd}\cdot i_{sq} - \psi_{rq}\cdot i_{sd}) \tag{3}$$

2.2. Modeling of IM in $(\alpha-\beta)$ reference frame

In a similar way, the mathematical model of an induction motor, expressed in the $(\alpha-\beta)$ stationary stator reference frame, is described by [14]:

$$\begin{cases} \frac{di_{s\alpha}}{dt} &= -\gamma i_{s\alpha} + \frac{K}{T_r}\psi_{r\alpha} + K.\omega_r\psi_{r\beta} + \frac{1}{\sigma L_s}v_{s\alpha} \\ \frac{di_{s\beta}}{dt} &= -\gamma.i_{s\beta} + K\omega_r\psi_{r\alpha} + \frac{K}{T_r}\psi_{r\beta} + \frac{1}{\sigma L_s}v_{s\beta} \\ \frac{d\psi_{r\alpha}}{dt} &= \frac{L_m}{T_r}i_{s\alpha} - \frac{1}{T_r}\psi_{r\alpha} - \omega_r\psi_{r\beta} \\ \frac{d\psi_{r\beta}}{dt} &= \frac{L_m}{T_r}i_{s\beta} - \omega_r\psi_{r\alpha} - \frac{1}{T_r}\psi_{r\beta} \end{cases} \tag{4}$$

3. Sliding mode control for IM

3.1. Rotor flux orientation

The entire control strategy depends on the correctness of the calibration of the reference frame (d-q), and thus on knowing the value of the angle of Park [14, 15].

$$\psi_{rq} = 0 \Longrightarrow \psi_r = \psi_{rd} \tag{5}$$

By imposing $\psi_{rq} = 0$, the model (1) becomes:

$$\begin{bmatrix} \frac{di_{sd}}{dt} \\ \\ \frac{di_{sq}}{dt} \end{bmatrix} = \begin{bmatrix} -\gamma i_{sd} + \omega_s i_{sq} + \frac{K}{T_r}\psi_r \\ -\omega_s i_{sd} - \gamma i_{sq} + K\omega_r\psi_r \end{bmatrix} + \begin{bmatrix} \frac{1}{\sigma L_s} & 0 \\ 0 & \frac{1}{\sigma L_s} \end{bmatrix} \begin{bmatrix} v_{sd} \\ v_{sq} \end{bmatrix} \tag{6}$$

and

$$\begin{cases} \frac{\psi_r}{dt} = \frac{L_m}{T_r}.i_{sd} - \frac{1}{T_r}.\psi_r \\ \omega_{sl} = \frac{L_m}{T_r.\psi_r}.i_{qs} \\ \frac{d\omega_r}{dt} = \frac{3}{2}\cdot\frac{n_p^2.L_m}{L_r}\cdot\psi_r.i_{sq} - \frac{n_p}{J}\cdot T_l - \frac{B}{J}.\omega_r \end{cases} \tag{7}$$

After passing through Laplace transformation, we obtain expressions:

$$\begin{cases} \psi_r = \frac{L_m}{1+T_r s} i_{sd} \\ \\ T_e = \frac{3}{2}\cdot\frac{n_p.L_m}{L_r}.\psi_r i_{sq} \end{cases} \tag{8}$$

where the permanent regime is established. The procedure consists of solving numerically the following equation [14]:

$$\frac{d\theta_s}{dt} = \omega_r + \frac{L_m i_{sq}}{T_r \psi_r} \tag{9}$$

In steady state, Equation (8) gives $\psi_r = L_m.i_{sd}$. Thus, Equation (9) becomes:

$$\frac{d\theta_s}{dt} = \omega_r + \frac{i_{sq}}{T_r i_{sd}} \tag{10}$$

3.2. Super-twisting control

The super-twisting algorithm is part of sliding mode control. It is particularly used in second-order sliding modes. This algorithm was originally proposed by Levant [16] in the case where the system has a relative degree equal to 1 with respect to the sliding variable, called S. This algorithm was developed while preserving the main advantages of first-order sliding modes (robustness, convergence in finite time). It has the great advantage of eliminating chattering. The control law of the super-twisting algorithm [11, 16] may be expressed as:

$$U = V_1(t) + V_2(t) \tag{11}$$

with

$$\begin{cases} V_1(t) &= -K_1 \mid S \mid^r sign(S) \\ V_2(t) &= -K_2 \int sign(S) \end{cases} \tag{12}$$

where S is the switching function; K_1 and K_2 are positive constants; and r is defined as $0 < r < 1$ [16, 17]. The general scheme of a such controller is illustrated Figure 1. This strategy is applicable to the first-order

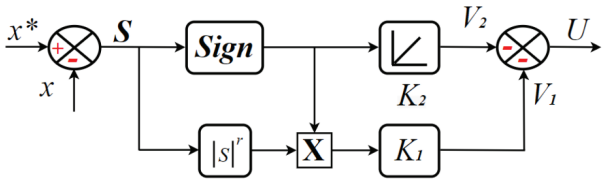

Figure 1. The general scheme of the super-twisting controller.

system. The relative degree of system (1) is $[i_{sd} \quad i_{sq} \quad \psi_{rd} \quad \psi_{rq} \quad \omega_r]^T = [1 \quad 1 \quad 2 \quad 2 \quad 2]^T$. In this study, the control strategy is designed by taking into account only the two variables $(\phi_{rd} = \phi_r, \quad \omega_r)$. The sliding surface S is defined as [18, 19]:

$$S = (\frac{d}{dt} + \lambda)^{r-1} e(x) \tag{13}$$

where e(x) stands for the variation of the variable to be regulated $(e(x) = x^* - x)$. Note that λ is a positive constant which represents the desired control bandwidth; r is the relative degree which is equal to the number of times required to derive the output in order to get the control input. The variables that need to be controlled are the rotor speed and rotor flux. The surface S is defined in a natural way as [16]:

$$S = \begin{bmatrix} S_{\psi_r} \\ S_{\omega_r} \end{bmatrix} = \begin{bmatrix} \dot{e}_{\psi_r} + \lambda_{\psi_r} e_{\psi_r} \\ \dot{e}_{\omega_r} + \lambda_{\omega_r} e_{\omega_r} \end{bmatrix} \tag{14}$$

The input of the control u in equation (11) is extended to u of equation (15), which can be written as:

$$u = \begin{bmatrix} V_{sd} & V_{sq} \end{bmatrix}^T \tag{15}$$

Then, one gets:

$$\dot{S} = \varsigma_1(.) + \varsigma_2(.)u \tag{16}$$

where the matrices ς_1 and ς_2 are given in the appendix. when $\dot{S} = 0$, the control input U may be expressed as:

$$u = [\varsigma_2(.)]^{-1}[-\varsigma_1(.) + \mu] \tag{17}$$

where μ is written as:

$$\mu = \begin{bmatrix} -K_1 \mid S_{\psi_r} \mid^r sign(S_{\psi_r}) - K_2 \int sign(S_{\psi_r}) \\ -K_3 \mid S_{\omega_r} \mid^r sign(S_{\omega_r}) - K_4 \int sign(S_{\omega_r}) \end{bmatrix} \tag{18}$$

where K_1, K_2, K_3, and K_4 are positive constants of the super-twisting controllers of the rotor speed and rotor flux [19, 20].

Figure 2 shows the full system structure, with the super-twisting control and the rotor flux orientation, the proposed observer, as well as the fuzzy detection and reconfiguration system. For more details on the estimator block see Figure 3 and the details of the fuzzy decision and reconfiguration is given later (please see Section 5): The role of the estimator block (Figure 3) consists of aligning the direct axis (d) of the (d-q) Reference frame on the rotor flux so $\psi_{rq} = 0 \Longrightarrow \psi_r = \psi_{rd}$.

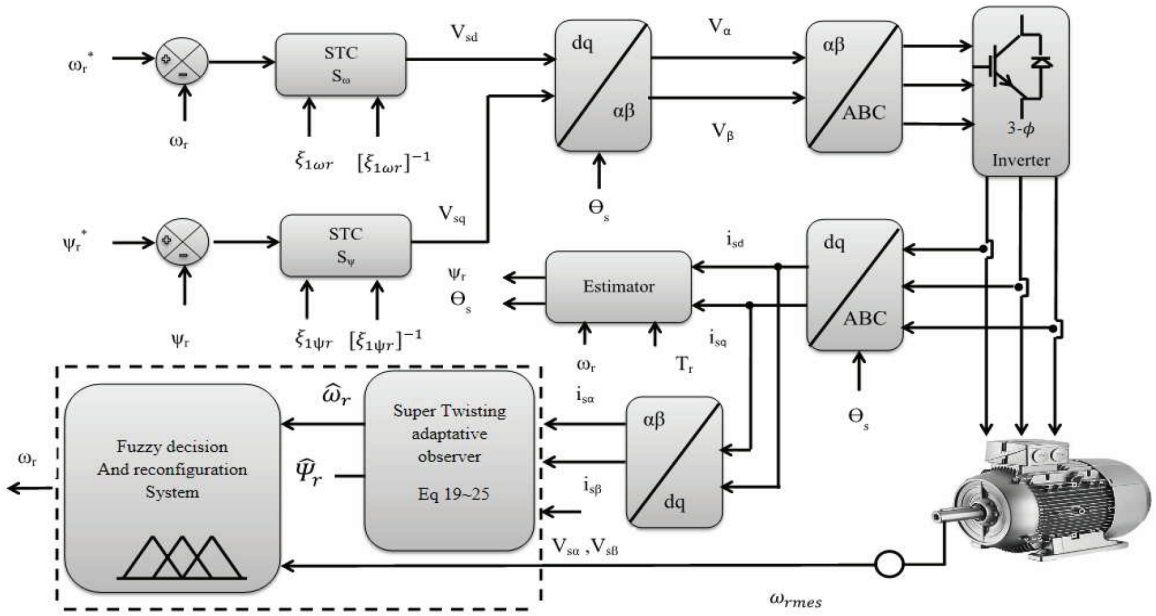

Figure 2. Block diagram of the IM drive system with the proposed sensor fault detection and reconfiguration system.

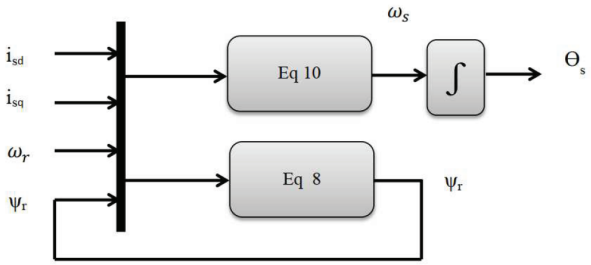

Figure 3. Block diagram of Park angle and rotor flux estimator.

4. Model of the rotor speed observer

The observer proposed in this article is a new hybrid observer close to the sliding observer; its role is to estimate the rotor fluxes in the stationary frame of reference $(\alpha - \beta)$ while ensuring the convergence of the observer of the current in the same reference frame. Once the flux values are found, they are used in the adaptive observer and the super-twisted sliding mode observer in order to estimate rotor speed. The approach used here is well detailed in what follows. For clarity, model (4) can be written as [21]:

$$\begin{cases} \frac{di_{s_\alpha}}{dt} &= -\gamma i_{s\alpha} + \frac{K}{T_r}\psi_{r\alpha} - K\omega_r\psi_{r\beta} + \frac{1}{\sigma L_s}v_{s\alpha} + K_c S_{i\alpha} + K_v sign(S_{i\alpha}) \\ \frac{di_{s_\beta}}{dt} &= -\gamma . i_{s\beta} + K\omega_r\psi_{r\alpha} + \frac{K}{T_r}\psi_{r\beta} + \frac{1}{\sigma L_s}v_{s\beta} + K_c S_{i\beta} + K_v sign(S_{i\beta}) \\ \frac{d\psi_{r_\alpha}}{dt} &= \frac{L_m}{T_r}i_{s\alpha} - \frac{1}{T_r}\psi_{r\alpha} - \omega_r\psi_{r\beta} + K_\psi sign(S_{i\alpha}) \\ \frac{d\psi_{r_\beta}}{dt} &= \frac{L_m}{T_r}i_{s\beta} - \omega_r\psi_{r\alpha} - \frac{1}{T_r}\psi_{r\beta} + K_\psi sign(S_{i\beta}) \end{cases} \quad (19)$$

Where

$$\begin{bmatrix} S_{i\alpha} \\ S_{i\beta} \end{bmatrix} = \begin{bmatrix} e_{i_{s\alpha}} \\ e_{i_{s\beta}} \end{bmatrix} = \begin{bmatrix} \hat{i}_{s\alpha} - i_{s\alpha} \\ \hat{i}_{s\beta} - i_{s\beta} \end{bmatrix} \tag{20}$$

$S_{i_{s\alpha,\beta}}$ are sliding mode surfaces and K_c, K_v, and K_ψ are the observer gains. The convergence of the estimated currents $\hat{i}_{s\alpha}$ and $\hat{i}_{s\beta}$ towards the real stator currents $i_{s\alpha}$ and $i_{s\beta}$ makes it possible to estimate the rotor fluxes $\hat{\psi}_{r\alpha}$ and $\hat{\psi}_{r\beta}$ which allow evaluating the rotor speed with the adaptive observer using a super-twisting-based strategy [21].

4.1. Observer based on adaptive super-twisting strategy

4.1.1. Adaptive observer

The speed estimation method using an adaptive observer is an approach known for the simplicity of its algorithm, its stability, and rapid convergence, as well as for its performance in terms of accuracy in a fairly wide speed range. The adaptation law obtained to ensure the convergence of $\hat{\omega}_r$ to ω_r is of type proportional-integral; it is expressed by means of the following relation [22]:

$$\hat{\omega}_r = K_p(e_{i_{s\alpha}}\hat{\psi}_{r\beta} - e_{i_{s\beta}}\hat{\psi}_{r\alpha}) - K_i \int (e_{i_{s\alpha}}\hat{\psi}_{r\beta} - e_{i_{s\beta}}\hat{\psi}_{r\alpha}) \tag{21}$$

with K_p , K_i are respectively the proportional and integral gains and

$$\begin{bmatrix} e_{i_{s\alpha}} \\ e_{i_{s\beta}} \end{bmatrix} = \begin{bmatrix} \hat{i}_{s\alpha} - i_{s\alpha} \\ \hat{i}_{s\beta} - i_{s\beta} \end{bmatrix}$$

The main disadvantage of this technique is that the estimate is less accurate at low speeds. For this reason it was decided to use the super-twisting technique [22, 23].

4.1.2. Adaptive super-twisting observer

In this section, the PI regulator is replaced by a super-twisting controller in order to guarantee a better estimation of the rotor speed over all low speeds. The super-twisting algorithm does not require any information on the value of s (and hence its great practical interest) while retaining good robustness properties. The control law using the super-twisting algorithm may therefore be written just like equation (11) [16, 19, 24]. Consequently:

$$U = V_1(t) + V_2(t) \tag{22}$$

with

$$\begin{cases} V_1(t) &= -\lambda_i \mid S \mid^r sign(S) \\ V_2(t) &= -\lambda_p \int sign(S) \end{cases} \tag{23}$$

where

$$S = e_{i_{s\alpha}}\hat{\psi}_{r\beta} - e_{i_{s\beta}}\hat{\psi}_{r\alpha} \tag{24}$$

Thus,

$$\hat{\omega}_r = -\lambda_i \mid S \mid^r sign(S) - \lambda_p \int sign(S) \tag{25}$$

5. Speed sensor fault tolerant control

This section focuses on the fault-tolerant control method that relies on the speed estimate obtained by means of the suggested adaptive super-twisting observer. The measured and estimated speeds are fed into the fuzzy detection and decision unit in order to detect and reconfigure the faulty speed sensor based on the estimated speed [11, 25]. The estimation of speed is not influenced by the speed sensor fault. For fault identification, it is reasonable to write:

$$e_{\omega r} = \omega_r - \hat{\omega}_r \tag{26}$$

5.1. Fuzzy detection and decision system

The fault-tolerant control system is displayed in Figure 4. The fault in our case results from a speed sensor failure. The transition of the command by super-twisting, using the speed sensor, towards the adaptive super-twisting observer (sensorless control) must ensure the continuity of operation of the system, which in turn guarantees the continuity of the IM control.

The basic idea is to develop a transition block capable of generating a transition function U_{Tr}; this function is defined as a linear combination of the speed measured by the sensor and the speed delivered by the proposed observer.

$$U_{Tr} = (1 - F_s)\omega_r + F_s\hat{\omega}_r \tag{27}$$

- F_s: Transition function obtained from the block based on fuzzy logic.
- $F_s = 0$ there is no problem.
- $F_s = 1$ there is a problem.

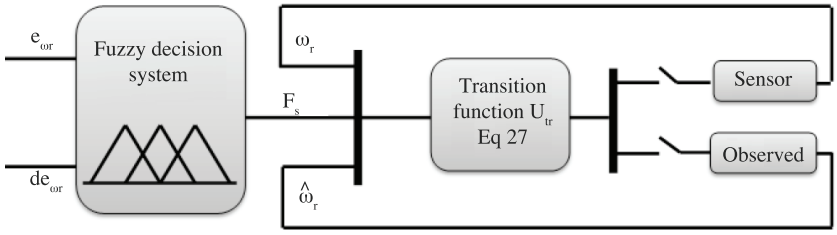

Figure 4. Architecture of the fault-tolerant controller.

5.1.1. Fuzzy decision block design

The fuzzy decision block receives the two input variables, e and de , and delivers the output variables F_s:

$$\begin{cases} e_{\omega r} &= \omega_r - \hat{\omega}_r \\ \frac{de_{\omega r}}{dt} &= \frac{d}{dt}(\omega_r - \hat{\omega}_r) \end{cases} \tag{28}$$

5.1.2. Fuzzy rules extraction

A Mamdani-type fuzzy implementation using a max-min inference was chosen. The membership functions describe the variable along a normalized universe of discourse. The fuzzy variables can be negative great (NG), close to zero (Z), and positive great (PG), as can be seen in Figure 5 [2, 13]. To make things clearer, some rules are described below:

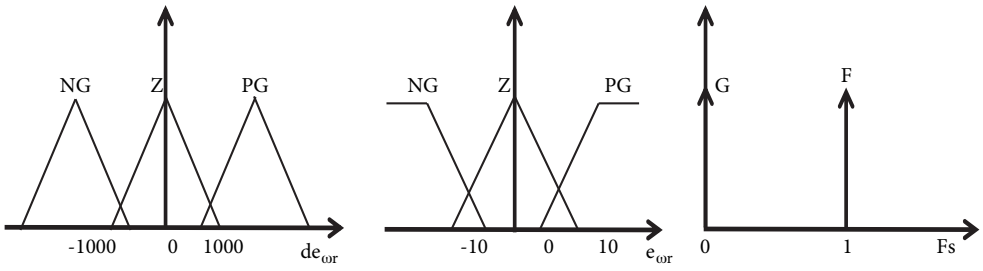

Figure 5. Distribution of membership functions of the input/output variables: **Left**-function of speed error derivative. **Middle**-function of speed error. **Right**-function of fault detector.

- If ($e\omega_r$ is NG or PG) and ($de\omega_r$ is NG or PG), then (F_s is F). The extracted rule suggests that in the case where ΔIs and the error on the speed are negative great (NG) or positive great (PG), then the quantity Fs (fault detector) is equal to F in this case, and the observer is selected. Therefore, a failure in the speed sensor engenders a transition.

-If ($e\omega_r$ is Z) and ($de\omega_r$ is Z), then (F_s is G). In this case, no transition is made, which indicates that the speed sensor is working properly.

-If ($e\omega_r$ is Z) and ($de\omega_r$ is PG), then (F_s is G). In this case, no transition is made since the information on the speed (e null) indicates that the speed sensor is working properly.

6. Simulation results

In order to test the validity of the controller, simulations were implemented by means of the Matlab / Simulink software package, for a sample time step T = 10^{-5}s. It is important to mention that the nominal model of the induction motor and all the constraints to which it is subjected were taken into account. First, the actuator faults are introduced at $t = 2s$, and then the fault-tolerant control, with and without the load torque, is studied. It should be noted that the defect may be the result of a cable break, which means that no information can be obtained from the rotor speed sensor. The results obtained are presented in the following figures. In order to assess the performance and robustness of the speed sensor fault detection method, it was decided to conduct the following two scenarios:

1- Appearance of speed sensor defect at no load.

2- Appearance of speed sensor defect with load torque.

The benchmark was chosen to test the reaction of the fuzzy decision and reconfiguration block at high speeds and reverse speeds.

6.1. Scenario 1

This scenario was devised to see the performance of the system without the application of the load torque but in the presence of the speed sensor fault, as shown in Figure 6.

Figure 6 presents the simulation results of the induction machine under super-twisting control, with a defect on the speed sensor at $t = 2$ s. It is expected to find the rotor flux at $t = 0.2$ s, for the zero reference speed ($\omega_r^* =$). Moreover, it is important to note that after a reference change from 0 to 120 rad/s and a reversal of the speed to –120 rad/s at $t = 3$ s, the rotor speed r responds very quickly, thanks to the properties of super-twisting control; in this case, the convergence occurs in a finite time. When the fuzzy decision system detects the fault, the speed sensor fault ($Fs = 1$) is observed at $t = 2$ s. The transition to the adaptive

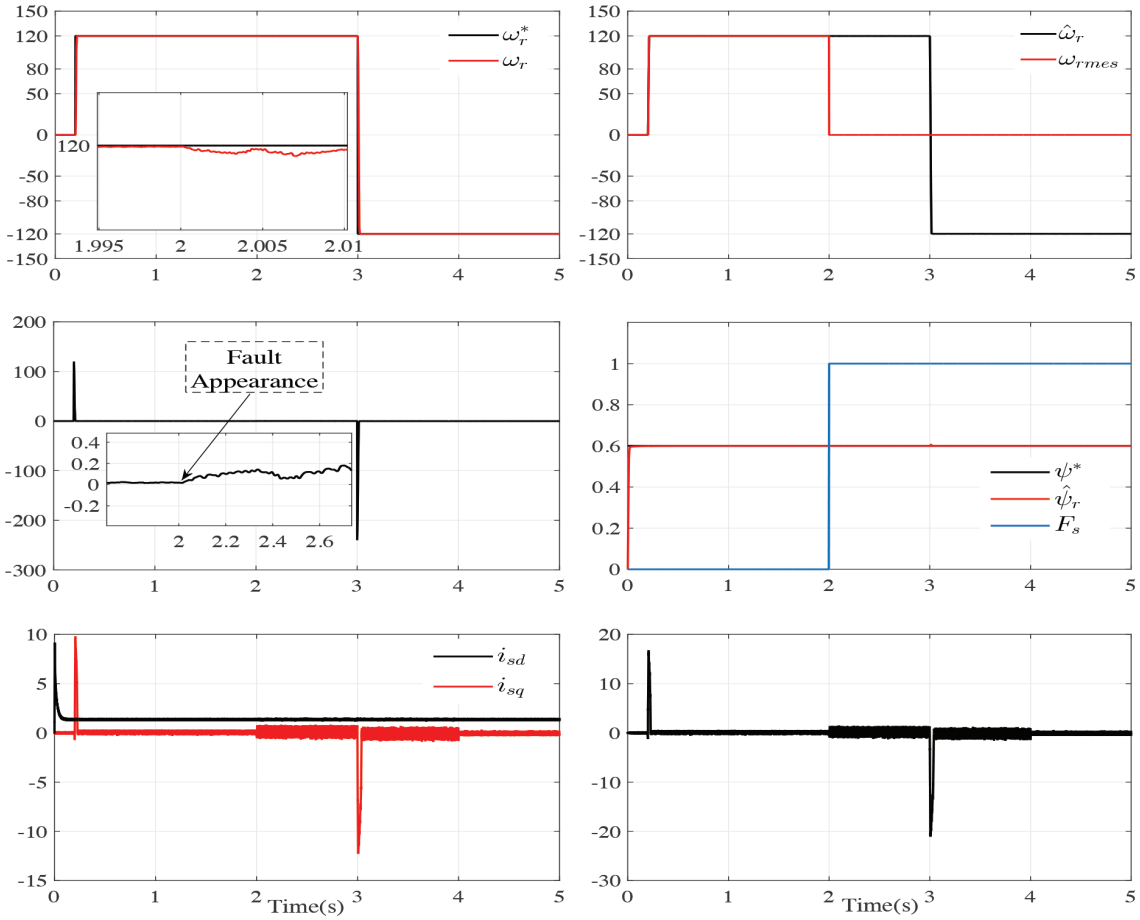

Figure 6. Performance of speed sensor fault tolerant control at no load- **Top-left**- Rotor speed (rad/s) versus time (s). **Top-right**- Estimated and measured rotor speed (rad/s) versus time (s). **Middle-left**- Error of speed estimation (rad/s) versus time (s). **Middle-Right**- Rotor flux (Wb) nad transition function versus time (s). **Bottom-left**- Stator currents in d-q axis (A) versus time (s). **Bottom-Right**- Electromagnetic torque (Nm) versus time (s).

super-twisting observer ensures a very good continuity of service of the system thanks to a good estimation of the rotor speed and rotor flux. It can clearly be seen that the difference between the reference speed (ω_r^*) and the controlled speed (ω_r) is negligible even at the appearance of the default. The current (i_{sd}) is not perturbed by the large changes in the current (i_{sq}). Therefore, the simulation proves the presence of a decoupling of the vector control. Moreover, there is a small noise in the current (i_{sq}) when the defect appears and this is certainly due to the chattering that exists in the estimated speed by the proposed observer. The electromagnetic torque (T_e) is almost zero because there is no applied load torque except there is noise when the speed sensor fault occurs. The electromagnetic torque is the image of the stator current (i_{sq}).

6.2. Scenario 2

It is the same test as the previous scenario but with the application of the load torque to see the reaction of the detection and reconfiguration system. When the same benchmark is used along with an application of the load torque at $t = 1$ s, the results of the simulation in Figure 7 are found identical to those in Figure 6.

The only difference is that there is an increase in the stator current (i_{sq}) and the electromagnetic torque (T_e) because a load torque is applied at $t = [1, 4]$s so there is the call of the satator current (i_{sq}). The fuzzy failure detection and reconfiguration block does not give false alarms, despite the application of the load torque. On the other hand, with the appearance of the speed sensor fault $(F_s = 1)$ at $t = 2$ s, the transition to the adaptive super-twisting observer gives very good results while ensuring the continuity of service of the system.

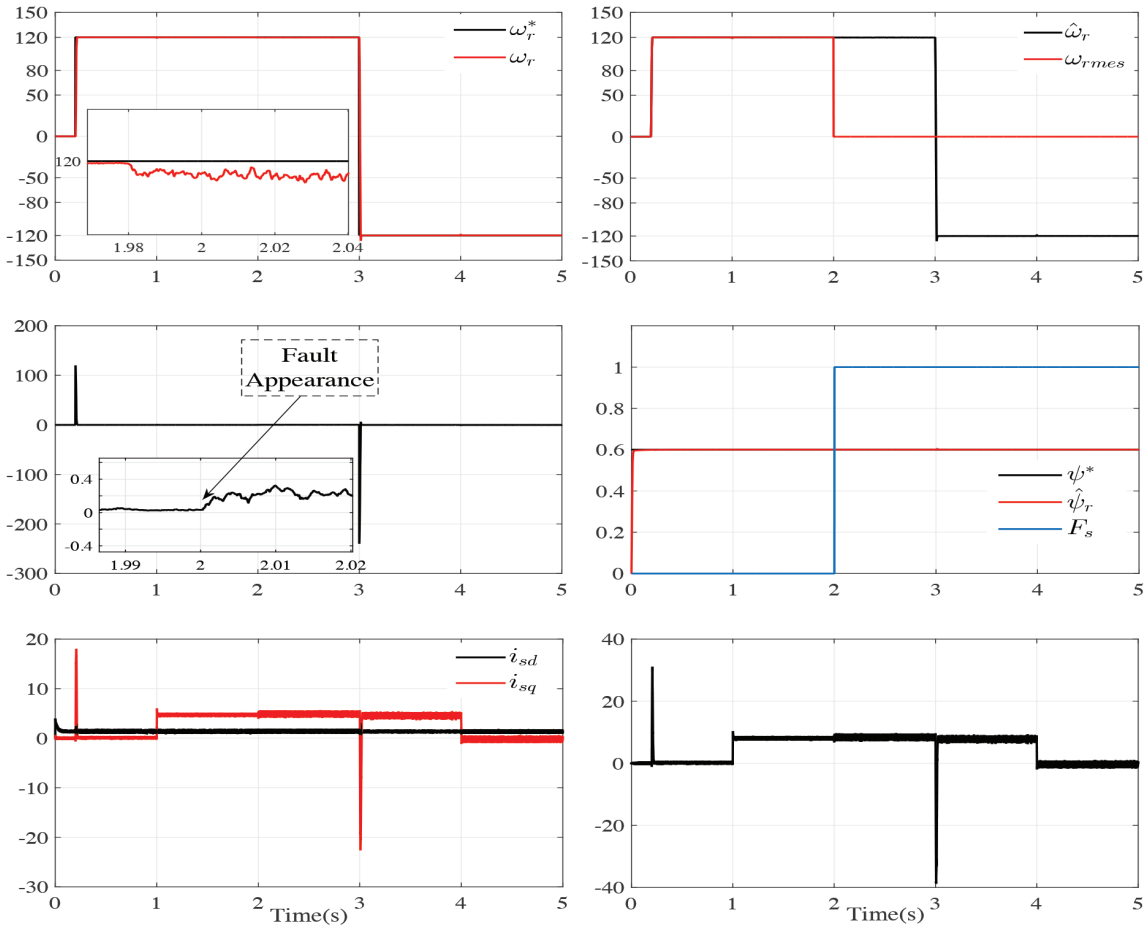

Figure 7. Performance of speed sensor fault-tolerant control with load torque. **Top-left**- Rotor speed (rad/s) versus time (s). **Top-right**- Estimated and measured rotor speed (rad/s) versus time (s). **Middle-left**- Error of speed estimation (rad/s) versus time (s). **Middle-Right**- Rotor flux (Wb) nad transition function versus time (s). **Bottom-left**- Stator currents in d-q axis (A) versus time (s). **Bottom-Right**- Electromagnetic torque (Nm) versus time (s).

6.3. Scenario 3

In order to demonstrate the effectiveness and the reaction of the proposed system in this paper at low speed and in the nonobservability zone $(\omega_s = 0)$, we choose this benchmark with the presence of the speed sensor fault at $t = 2$ s, the fault in this case, and with the sensor giving false information. In addition, we applied a load torque at $t = [1, 4]$ s and we got these results: Figure 8 shows the performance of the proposed system at low speed and in the nonobservability zone. The rotor speed correctly follows its reference even with the appearance of the fault at $t = 2$ s so $F_s = 1$ and application of a load torque of $T_l = 8$ Nm at $t = [1, 4]$ s, and

the error of the rotor speed is negligible $(e_{\omega r})$. The estimated flux $(\hat{\psi}_r)$ follows its reference (ψ_r^*) and this is thanks to the proposed observer. A little noise on the (i_{sq}) current is seen when the fault appears and even on the electromagnetic torque (T_e) because of the information on the rotor speed provided by the observer is a little noisy (area of nonobservability). The results presented in this scenario show very well the reliability and robustness of the system and this is thanks to the robustness of the observer and the system of detection and reconfiguration proposed in this paper.

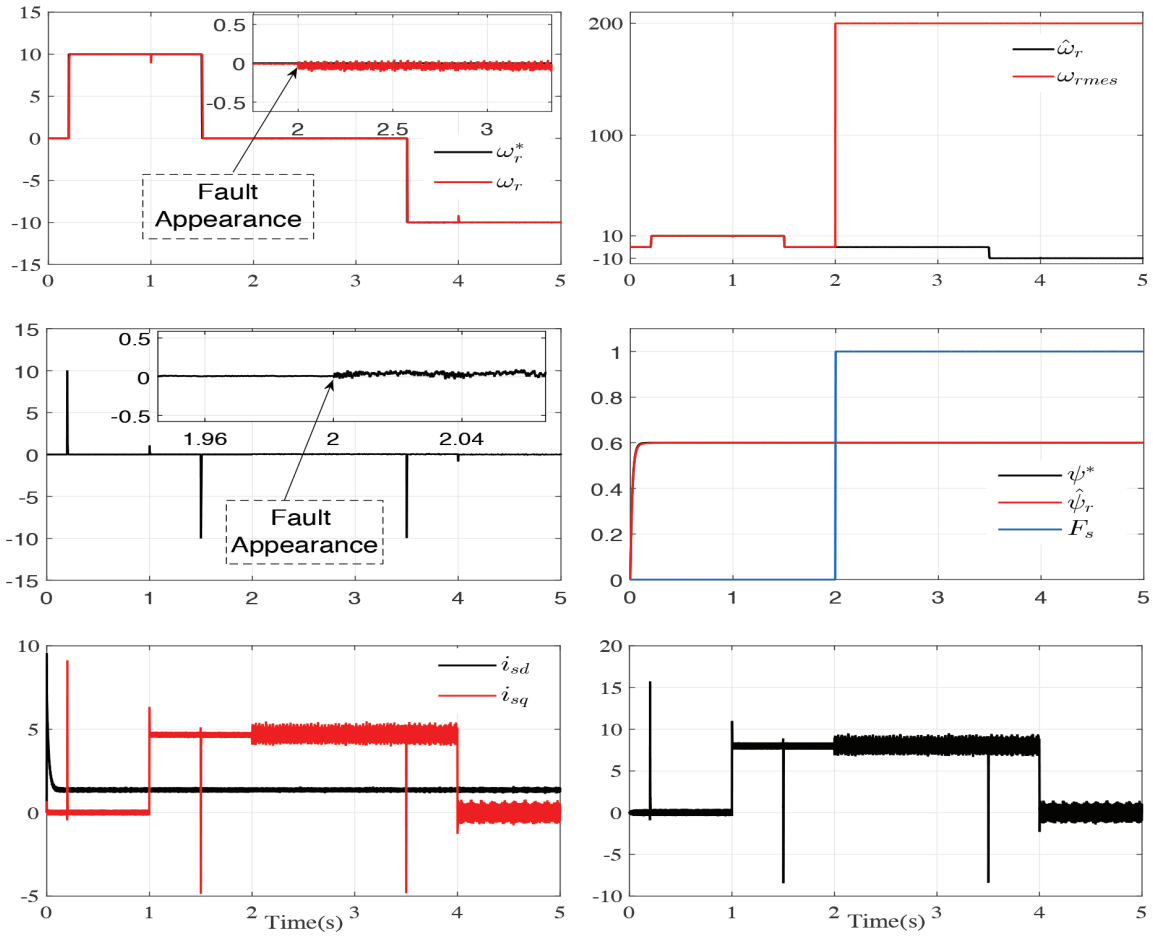

Figure 8. Performance of speed sensor fault-tolerant control with load torque at low speed. **Top-left**- Rotor speed (rad/s) versus time (s). **Top-right**- Estimated and measured rotor speed (rad/s) versus time (s). **Middle-left**- Error of speed estimation (rad/s) versus time (s). **Middle-Right**- Rotor flux (Wb) nad transition function versus time (s). **Bottom-left**- Stator currents in d-q axis (A) versus time (s). **Bottom-Right**- Electromagnetic torque (Nm) versus time (s).

6.4. Scenario 4

Robustness tests were carried out in order to examine the reaction and robustness of the fuzzy supervisor and the proposed reconfiguration system. The values of resistances R_s and R_r were varied in the tests, while a load torque was applied; the default appeared at $t = 2$ s. The values of resistances R_s and R_r were appropriately chosen because the variation of Rs influences the controller and the variation of R_r influences the observer.

The tests are presented hereafter:
Tests 1: $R_s = (1 + 20\%).R_{sn}$, $R_r = R_{rn}$.
Test 2: $R_s = R_{sn}$, $R_r = (1 + 20\%).R_{rn}$.
Tests 3: $R_s = (1 + 20\%).R_{sn}$, $R_r = (1 + 20\%).R_{rn}$.
Tests 4: $R_s = (1 + 50\%).R_{sn}$, $R_r = (1 + 50\%).R_{rn}$. Figures 9–12 present good results, thanks to the super-twisting command, with convergence of ω_r to ω_r^*, in a finite time. The adaptive super-twisting observer guarantees the continuity of the system when there is a transition after the appearance of the defect at $t = 2$ s. The rotor speed (ω_r) follows its reference (ω_r^*) with the presence of the speed sensor fault and even with the variations of the stator and rotor resistances. The error of rotor speed $(\omega_r^* - \omega_r)$ is negligible during the entire simulation range. In addition, the fuzzy supervisor is robust to parametric variations, for the variations of R_s and R_r separately, and for the variations of both at the same time. This robustness persists even with the application of the load torque; it shows excellent sensitivity to speed sensor defects.

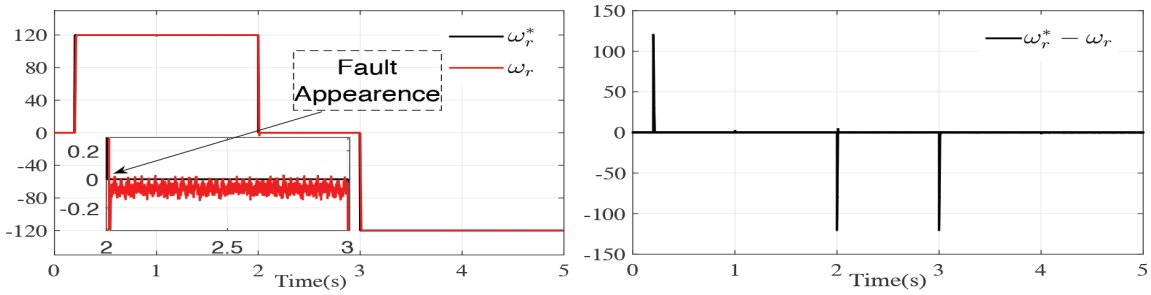

Figure 9. Speed sensor fault-tolerant controller $R_s = (1 + 20\%).R_{sn}$, $R_r = R_{rn}$. **Left**- Rotor speed (rad/s) versus time (s). **Right**- Error of rotor speed (rad/s) versus time (s).

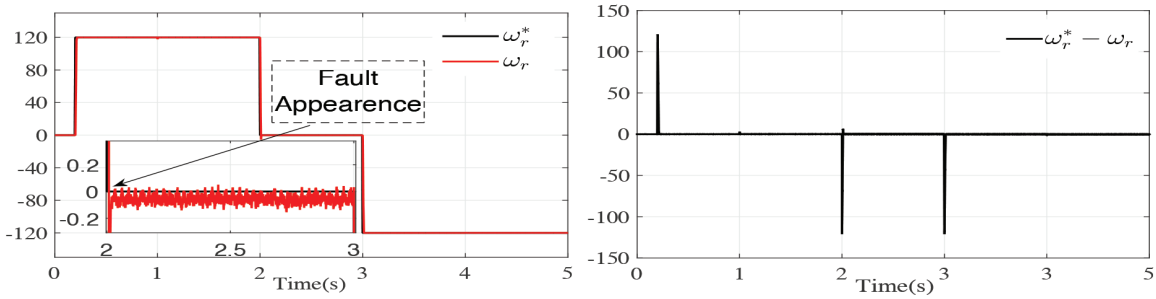

Figure 10. Speed sensor fault-tolerant controller R_{sn}, $R_r = (1+20\%).R_{rn}$. **Left**- Rotor speed (rad/s) versus time (s). **Right**- Error of rotor speed (rad/s) versus time (s).

6.5. Scenario 5

A comparison was made in this section to evaluate the proposed strategy with standard sliding mode (first order) with the benchmark used in scenario 2. In order to show clearly the difference between the two strategies used, Table summarizes the main performances.
Namely the standard deviation (STD) and the mean value of the rotor speed error (e_{ω_r}), stator currents (i_{sd})

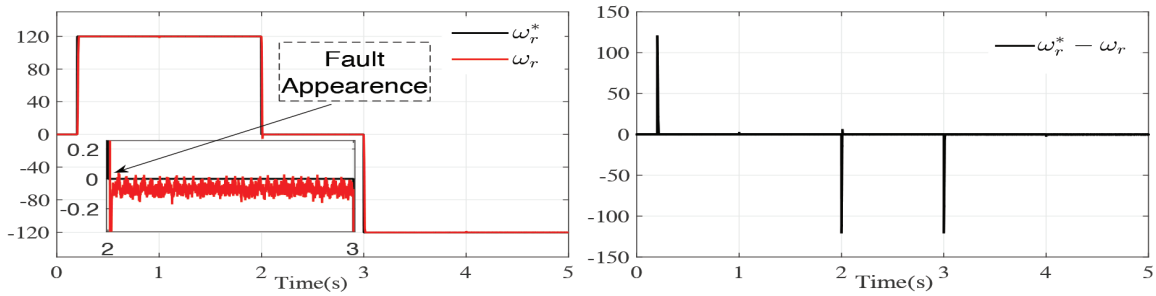

Figure 11. Speed sensor fault tolerant controller $R_s = (1+20\%).R_{sn}$, $R_r = (1+20\%).R_{rn}$. **Left**- Rotor speed (rad/s) versus time (s). **Right**- Error of rotor speed (rad/s) versus time (s).

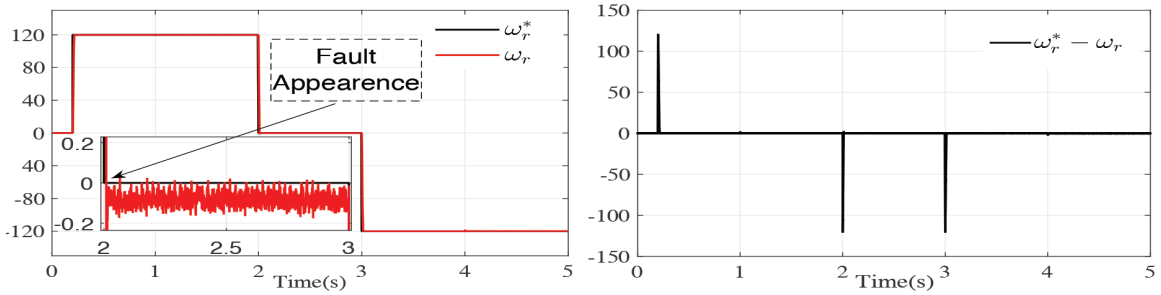

Figure 12. Speed sensor fault tolerant controller $R_s = (1+50\%).R_{sn}$, $R_r = (1+50\%).R_{rn}$. **Left**- Rotor speed (rad/s) versus time (s). **Right**- Error of rotor speed (rad/s) versus time (s).

and (i_{sq}), and electromagnetic torque (T_e). It should be noted that these indicators were collected over the entire simulation range.

Table . Performance comparison of the controllers.

Control strategy	Strategy 1	Strategy 2	Evaluation Strategy 2/Strategy 1
STD e_{ω_r}(rad/s)	5.3953	3.6428	–32.49%
STD i_{sd} (A)	0.4311	0.2763	–35.91%
STD i_{sq} (A)	2.6648	2.3931	–9.51%
STD T_e (Nm)	4.5335	4.1029	–9.5%
mean e_{ω_r} (rad/s)	1.8670	0.2387	–87.22%
mean i_{sd} (A)	1.3935	1.3877	–0.42%
mean i_{sq} (A)	3.1759	2.9369	–7.53%
mean T_e (Nm)	7.1589	5.0337	–29.69%

As explaned below, the STD and the mean values are calculated for the proposed method and the standard sliding mode. For a such comparison, the following notations will be used:

- Strategy 1 = standard sliding mode controller + adaptive standard sliding mode observer.
- Strategy 2 (proposed method) = super twisting controller + adaptive super twisting observer.

The STD of the variables are lower for Strategy 2 (proposed method). The reduction is significant -32.49% for error of rotor speed e_{ω_r}, -35.91% for the stator current i_{sd}. Concerning the mean value there is a significant reduction for error of rotor speed e_{ω_r} -87.22%, -29.69% for electromagnetic torque T_e. This last can be considered an indication for reducing the torque oscillations. The results show very well the advantage of the proposed method.

7. Conclusion

The present paper proposes a new sensor fault detection and isolation system with a reconfiguration algorithm for an induction motor based on a robust adaptive super-twisting observer. It is intended to maintain continuous system operation. Simulation results are presented to highlight the performance of the proposed approach and to show the robustness of the fuzzy supervisor to the parametric variations. The suggested method shows a great sensitivity in the event of a defect in the speed sensor. This is the main purpose of the detection and reconfiguration system proposed here. The proposed strategy (control+ observer) is compared to a standard sliding mode (control + observer), by considering the scenario 2, through some performance indicators as standard deviation and mean values. As future work, the authors will concentrate on the stability study in closed loop of the full system. An important next step will concern the experimental tests of the proposed strategy by taking into account the low-speed and zero-speed areas.

Appendix

Motor parameters

Rated values:

1.5 kW, 220/380 V, 6.3/3.5 A, 50 Hz, 2 poles, 1430 rpm

Rated parameters:

R_s=5.72 Ω, R_r=4.2 Ω, L_s=0.462 H, L_r=0.462 H, L_m=0.440 H, J=0.049 kg m^2, B=0.003 kg m/s.

Nomenclature

The matrices $\xi_1(.)$ and $\xi_2(.)$ are read as:

$$\xi_1 = \begin{bmatrix} \ddot{\psi_r}^* + \lambda_{\psi_r}\dot{\psi_r}^* + a_1\dot{\psi_r} + a_2 i_{sd} - a_3 i_{sq} - a_4\psi_r \\ \ddot{\omega_r}^* + \lambda_{\omega_r}\dot{\omega_r}^* + a_5\dot{\omega_r} + a_6\omega_s i_{sd} + (a_7 + a_{10})i_{sq} + a_8\omega_r - a_9 i_{sd} i_{sq} \end{bmatrix}; \xi_2 = \begin{bmatrix} \frac{L_m}{T_r\sigma L_s} \\ \\ \frac{K}{\sigma L_s}\psi_r \end{bmatrix}$$

where

$$a_1 = \frac{1}{T_r} - \lambda_{\psi_r}; \quad a_2 = \frac{L_m\gamma}{T_r}; \quad a_3 = \frac{L_m\omega_s}{T_r}; \quad a_4 = \frac{L_m K}{T_r^2}; \quad a_5 = \frac{Bn_p}{J} - \lambda_{\omega_r}$$

$$a_6 = K\psi_r; \quad a_7 = a_6\lambda; \quad a_8 = a_6\psi_r B; \quad a_9 = a_4 T_r; \quad a_{10} = \frac{a_6}{T_r}$$

$_{r}$, $_{s}$	subscripts for rotor and stator
$_{d}$, $_{q}$	subscripts for d and q axis
$_{\alpha}$, $_{\beta}$	subscripts for α and β axis
$_{n}$	subscript for nominal value
V ,i	voltage and current
ψ , ψ_{rn}	flux and nominal value of rotor flux
R_s , R_r	stator and rotor resistances
L_m	mutual inductance
L_s , L_r	stator and rotor inductances
T_s , T_r	stator and rotor time constant
σ	total leakage factor
J	moment of inertia
B	friction coefficient
n_p	number of pole pairs
T_e	electromagnetic torque
T_l	load torque
θ_s	position of rotor flux
ω_r	electrical angular rotor speed
ω_s	synchronously rotating angular speed
ω_{sl}	slip rotating angular speed
Ω_r	rotor mechanical angular speed
ω_r^*, ω_{rmes}	reference and musured rotor speeds
$\hat{\omega}_r$, $\hat{\psi}_r$	estimated rotor speed and estimated rotor flux
ψ, ψ^*	flux and its reference

Acknowledgment

The authors wish to thank the managers and members of the "Laboratoire d'Automatique de Tlemcen (LAT)" at the University of Tlemcen in Algeria for their precious remarks and suggestions and we thank the DGRSDT for their support.

References

[1] Benbouzid MEH, Diallo D, Zeraoulia M. Advanced fault tolerant control of induction-motor drives for EV/HEV Traction Applications. IEEE Transactions 2007; 56 (2): 519- 528. doi: 10.1109/TVT.2006.889579

[2] Baghli L, Poure P, Rezzoug A. Sensor fault detection for fault tolerant vector controlled induction machine. In: European Conference on Power Electronics and Applications, IEEE Energy Conversion Congress and Applications; Dresden, Germany; 2005; pp. 1-10.

[3] Gundewar SK, Kane PV. Fuzzy FMEA analysis of induction motor and overview of diagnostic techniques to reduce risk of failure. Reliability, Safety and Hazard Assessment for Risk-Based Technologies 2020; 1: 927-939. doi: 10.1007/978-981-13-9008-1_78

[4] Ali MZ, Shabbir MNSK, Kawsar Zaman SM, Liang X. Single- and multi-fault diagnosis using machine learning for variable frequency drive-fed induction motors. IEEE Transactions on Industry Applications 2020; 1: 1-20. doi: 10.1109/TIA.2020.2974151

[5] Hajary A, Kianinezhad R, Seifossadat SG, Mortazavi SS, Saffarian A. Detection and localization of open-phase fault in three-phase induction motor drives using second order rotational park transformation. IEEE Transactions on Power Electronics 2019; 34 (11): 11241-11252. doi: 10.1109/TPEL.2019.2901598

[6] Yetgin MG. Effects of induction motor end ring faults on motor performance. Experimental results. Engineering Failure Analysis 2019; (96): 374-383. doi: 10.1016/j.engfailanal.2018.10.019

[7] Pilloni A, Pisano A, Usai E. Robust FDI in induction motors via second order sliding mode technique. In: 12th IEEE Workshop on Variable Structure Systems; Mumbai, India; 2012. pp. 467- 472.

[8] Diao S, Diallo D, Makni Z, Marchand C. Diagnostic des capteurs pour la commande des entrainements électriques. In: Symposium de G´enie Electrique (SGE'14) : EF-EPF-MGE 2014; ENS Cachan, France; 2014. pp.1-20 (in French).

[9] Najafabadi TA, Salmasi FR, Jabehdar MP. Detection and isolation of speed-, DC-link voltage-, and current-sensor faults based on an adaptive observer in induction motor drives. IEEE Transactions on Industrial Electronics 2011; 58 (5): 1662-1672. doi: 10.1109/TIE.2010.2055775

[10] Krishna M, Daya F. Luenberger observer-based sensor fault detection: online application to DC motor. Turkish Journal of Electrical Engineering & Computer Sciences 2014; 22 (2): 363-370. doi: 10.3906/elk-1203-84

[11] Kommuri SK, Veluvolu KC, Defoort M. Second-order sliding mode based sensor fault-tolerant control of induction motor drives. In: International Conference on Industrial Instrumentation and Control (ICIC)College of Engineering; Pune, India; 2015. pp.1-20.

[12] Ortaç Kabaoglu R. A fault detection, diagnosis, and reconfiguration method via support vector machines. Turkish Journal of Electrical Engineering & Computer Sciences 2015; 23 (2): 589-601. doi: 10.3906/elk-1301-96

[13] Omaç Z. Fuzzy-logic-based robust speed control of switched reluctance motor for low and high speeds. Turkish Journal of Electrical Engineering & Computer Sciences 2019; 27 (1): 316-329. doi: 10.3906/elk-1712-186

[14] Vas P. Vector Control of AC Machines. USA: Oxford University Press, 1990

[15] Saleem A, Soliman H, Al-Ratrout S, Mesbah M. Design of a fractional order PID controller with application to an induction motor drive. Turkish Journal of Electrical Engineering & Computer Sciences 2018; 26 (5): 2768-2778. doi: 10.3906/elk-1712-183

[16] Levant A. Sliding order and sliding accuracy in sliding mode control. International Journal on Control 1993; 58 (6): 1247-1263. doi: 10.1080/00207179308923053

[17] Davila J, Fridman L, Levant A. Second-order sliding-mode observer for mechanical system. IEEE Transactions on Automatic Control 2005; 50 (11): 1785-1789. doi: 10.1109/TAC.2005.858636

[18] Utkin VI. Sliding Modes in Control and Optimization. USA: Springer Science & Business Media, 2013.

[19] Lascu C, Blaabjerg F. Super-twisting sliding mode direct torque control of induction machine drive. In: IEEE Energy Conversion Congress and Exposition (ECCE); Pittsburgh, PA, USA; 2014. pp. 5116-5122.

[20] Lascu C, Argeseanu A, Blaabjerg F. Super-twisting sliding mode direct torque and flux control of induction machine drives. IEEE Transactions on Power Electronics 2019; 35 (5): 5057-5065. doi: 10.1109/TPEL.2019.2944124

[21] Zhang X, Foo G, Vilathgamuwa MD, Tseng KJ, Bhangu BS et al. Sensor fault detection, isolation and system reconfiguration based on extended Kalman filter for induction motor drives. IET Electronic Power Applications 2013; 07 (7): 607- 617. doi: 10.1049/iet-epa.2012.0308

[22] Alkaya A, Eker I. Adaptive speed observer with disturbance torque compensation for sensorless induction motor drives using RT-Lab. Turkish Journal of Electrical Engineering & Computer Sciences 2016; 24 (5): 3792-3806. doi: 10.3906/elk-1502-198

[23] Salmasi FR, Najafabadi TA, Jabehdar MP. An adaptive flux observer with online estimation of DC-link voltage and rotor resistance for VSI-based induction motors. IEEE Transactions on Power Electronics, 2010; 25 (5): 1310-1319. doi: 10.1109/TPEL.2009.2038268

[24] Shtessel Y, Taleb M, Plestan P. A novel adaptive-gain super twisting sliding mode controller: Methodology and application. Automatica 2012; 48 (5): 1-20. doi: doi.org/10.1016/j.automatica.2012.02.024

[25] Dybkowski M, Klimkowski K. Speed sensor fault detection algorithm for vector control methods based on the parity relations. In: 19th European Conference on Power Electronics and Applications (EPE'17 ECCE Europe); Warsaw, Poland; 2017; 1-5.